WHEN DOES MOTION RELATIVE TO NEIGHBORING SURFACES ALTER THE FLOW THROUGH ARRAYS OF HAIRS?

C. LOUDON*, B. A. BEST† AND M. A. R. KOEHL

*Department of Integrative Biology, University of California at Berkeley, Berkeley,
CA 94720, USA*

Summary

Many animals from different phyla use structures bearing arrays of hairs to perform a variety of important functions, such as olfaction, gas exchange, suspension feeding and locomotion. The performance of all these functions depends on the motion of water or air around and through these arrays of hairs. Because organisms often move such hair-bearing appendages with respect to their bodies or the substratum, we assessed the effects of such motion relative to walls on the fluid flow between neighboring hairs. We compared flow fields near dynamically scaled physical models of hairs moving near walls with those calculated for such hairs in an unbounded fluid. Our results suggest that the methods an organism can use to change the flow through a hair-bearing appendage differ with Reynolds number (based on hair diameter). When Re is 10^{-2} or below, changing speed does not alter the proportion of the fluid that moves through rather than around the array, whereas moving relative to a wall increases it. In contrast, when Re is between 10^{-2} and 1, changes in speed have a big effect on the proportion of fluid moving through the array, while moving near walls makes little difference.

Introduction

Many animals from different phyla use structures bearing arrays of hairs to perform a variety of important functions, such as olfaction, gas exchange, suspension feeding, locomotion and ventilation (Fig. 1). In the case of olfactory antennae or gills, the hairs capture molecules from the surrounding water or air, while in the case of suspension-feeding appendages, the hairs harvest particles from the fluid. Hair-bearing appendages are also used by small animals to swim or fly through the surrounding medium or to move currents of water or air past their bodies. Therefore, the performance of the diverse functions served by different hair-bearing appendages all depends on the interaction of the appendage with the surrounding medium. Fluid can move around or through an array of hairs: a 'leaky' array can filter more fluid per time (to harvest molecules or particles) than a non-leaky one moving at the same velocity, whereas the non-leaky array might be

*Present address: Department of Entomology, Kansas State University, Manhattan, KS 66506, USA.
†Present address: Department of Biology, Colby College, Waterville, ME 04901, USA.
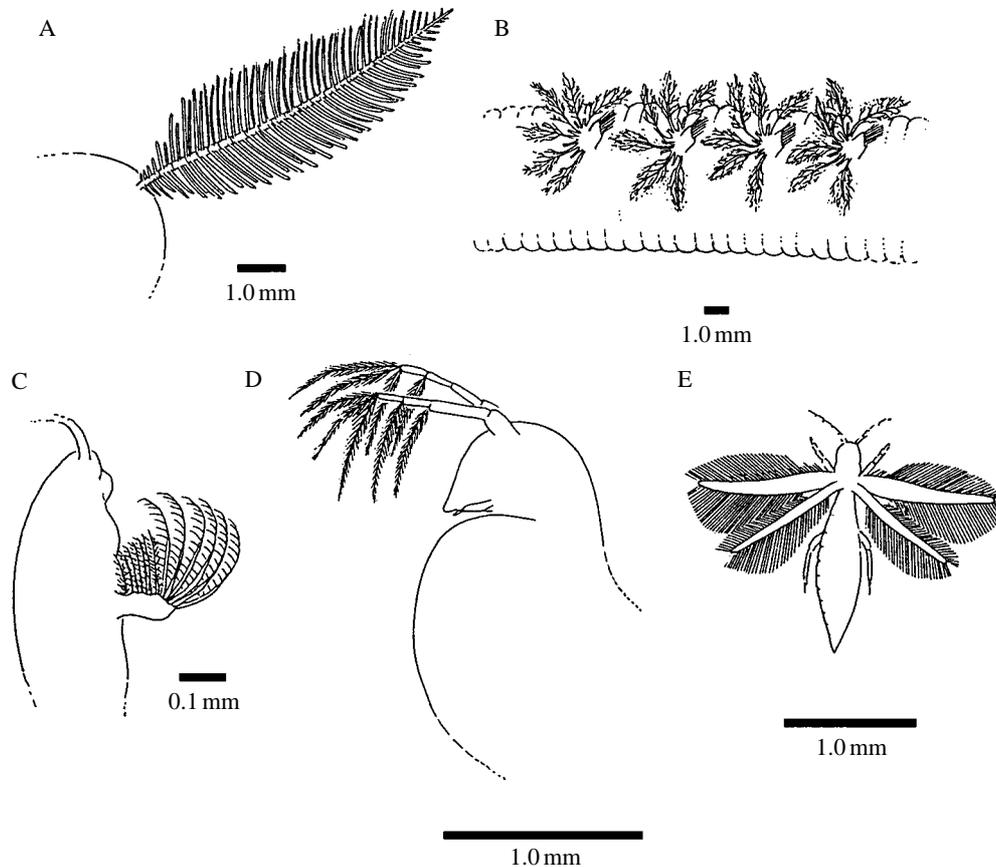
Fig. 1. Examples of appendages composed of arrays of cylinders that perform different physiological functions: molecule capture in (A) air (antenna of moth) and in (B) water (gill of polychaete worm), particle capture (C) in water (feeding appendage of copepod) and locomotion in (D) water (swimming appendage of cladoceran) and in (E) air (wing of thrips).

a more effective paddle (to propel fluid past the organism). Here, the term 'leakiness' is used as defined by Cheer and Koehl (1987a,b) to describe the volume of fluid passing through a gap between two cylinders in a unit of time divided by the volume of fluid moving at ambient velocity that would have passed through that same gap in the same period if the cylinders had not been there.

Arrays of hairs operating at low Reynolds numbers

The relative importance of inertial to viscous forces in determining the fluid flow around a body or a hair is represented by the Reynolds number (*Re*),

$$Re = LU/\nu, \tag{1}$$

where L is a characteristic linear dimension such as the diameter of a cylinder, U is the velocity of the fluid relative to the body, and ν is the kinematic viscosity of the fluid (i.e. $15 \times 10^{-6}\,\mathrm{m^2\,s^{-1}}$ for air and $1 \times 10^{-6}\,\mathrm{m^2\,s^{-1}}$ for fresh water, both at 20 °C; Vogel, 1981).

The hairs on a variety of filter-feeding and locomotory appendages operate at low Re values (10^{-5} to 10, based on hair diameter; reviewed in Rubenstein and Koehl, 1977; Jørgensen, 1983; LaBarbera, 1984; Cheer and Koehl, 1987b; Shimeta and Jumars, 1991). Similarly, sensory hairs on a variety of olfactory appendages operate at Re values of 10^{-4} to 10, although less information is available for these. This olfactory Re range is calculated from equation 1 using $2\,\mu$m and $20\,\mu$m for representative insect sensillum and crustacean aesthetasc diameters respectively (e.g. Ghiradella *et al.* 1968; Steinbrecht, 1970; Altner and Prillinger, 1980; Cheer and Koehl, 1987a) and ambient velocity ranges of 0.001–10 m s^{-1} for air (e.g. Gibson and Brady, 1985; Willis and Arbas, 1991; Willis *et al.* 1991; Srygley and Dudley, 1993) and 0.001–0.5 m s^{-1} for water (e.g. Moore *et al.* 1991; B. A. Best, unpublished data).

When a fluid moves relative to a solid body, the layer of fluid in contact with the surface of the body does not slip with respect to that surface; hence, a velocity gradient develops in the fluid between the surface and the freestream flow (boundary layer). The slower the flow, the thicker the boundary layer; at low Re values, this velocity boundary layer can be quite thick relative to the dimensions of the body. Flow at low Re is laminar (as described in White, 1946; Happel and Brenner, 1965; Vogel, 1981); hence, there is no turbulent mixing between adjacent fluid layers and molecular diffusion is the only mechanism that moves dissolved substances (e.g. odorants) across streamlines towards or away from the surface of a hair (e.g. a sensillum). Therefore, the rate of arrival of fluid-borne molecules at the surface of a hair depends first on the convection of the fluid to the vicinity of the hair and then on the diffusion from the bulk flow to the surface of the hair (DeSimone, 1981). Note that the convection in the vicinity of the hair will be a function of how much fluid passes through, rather than around, the array (the leakiness). Mathematical models of the diffusion of chemical signals to the surface of a sensory hair illustrate the importance of the velocity field around the hair to the rates at which molecules arrive at the hair's surface (e.g. Adam and Delbrück, 1968; Murray, 1977; Futrelle, 1984). Similarly, theory predicts that the mechanisms and rates of particle capture by filter-feeding appendages depend on the velocity profiles around the hairs of the filter (e.g. Rubenstein and Koehl, 1977; Spielman and Goren, 1977; Shimeta and Jumars, 1991). Nonetheless, velocity profiles or leakiness estimates for *finite arrays* of hairs (as opposed to a single cylinder or an infinitely wide row of cylinders) have not been available until recently for these biologically relevant Reynolds numbers (Cheer and Koehl, 1987b; Hansen and Tiselius, 1992; Koehl, 1992; Leonard, 1992).

Appendages, by definition, operate near a body to which they are attached and, hence, can move with respect to both the surface of the body and surfaces in their environments (such as the substratum or the walls of a burrow). Objects moving at low Re can be affected by walls that are quite far away; for example, walls must be 200 000 cylinder diameters away before they no longer influence the drag on a cylinder at $Re=10^{-4}$ (White, 1946). Since viscosity should retard the motion of a fluid relative to a wall, we might expect more fluid to be forced between the hairs of a low-Re appendage moving along or towards a wall than would flow between the hairs when moving in an unbounded fluid. In this paper, only the effects of arrays of hairs *moving* with respect to walls will be considered, although it should be kept in mind that, in some other cases, an array and the

nearby wall move together with respect to the surrounding fluid. Such walls moving with the hairs would be expected to have an opposite effect to that of stationary walls, i.e. to decrease rather than to increase the flow between hairs.

Dynamically scaled physical models of arrays of hairs

Dynamically scaled physical models provide a useful tool for studying the fluid motion around bodies that are too large or small to be conveniently manipulated or measured in the laboratory. If the model and the prototype are geometrically similar and are characterized by the same Re, then the ratios of the velocities and the forces at comparable positions in model and prototype are the same. Two recent studies have used such physical models to investigate fluid flow near arrays of hairs: Leonard (1992) and Hansen and Tiselius (1992) both used physical models consisting of a row of small cylinders of finite length attached at right angles to a larger cylinder. In both cases, the models were towed through tanks of fluid to yield the desired Re values (Re=1.7–197, Leonard, 1992; Re=0.04–40, Hansen and Tiselius, 1992). However, since walls can affect low-Re objects even when they are many diameters away, the sides and bottoms of the experimental tanks used in these studies may have altered the flow fields around models operating at the lowest Re values. Indeed, Hansen and Tiselius (1992) warned that the walls of the tank probably introduced artifacts into their measurements for Re values below 0.1.

Vogel (1981) provides a rule of thumb for estimating when wall effects can be safely ignored:

$$\frac{Y}{L} > \frac{20}{Re} = \frac{20v}{LU} \, , \tag{2}$$

where Y is the distance to the wall, L is the characteristic length of the body (e.g. cylinder diameter), U is the velocity of the body relative to the fluid and wall, and v is the kinematic viscosity of the fluid. For example, for Re=10^{-4}, to ensure no wall effects on the flow field around a single cylinder 2 mm in diameter, a towing tank 400 m wide would have to be used (containing 4×10^9 l of fluid). Clearly, wall effects must be addressed in experiments using physical models of low-Re objects conducted in tanks of more reasonable sizes.

Purpose and basic approach of this study

The purpose of our study was to explore the consequences of the presence of walls for the fluid flow between neighboring hairs. Our intent was twofold: (1) to determine the general circumstances in which motion relative to a wall might be expected to affect the flow through hair-bearing appendages, and (2) to assess the Reynolds numbers at which tank walls can introduce significant artifacts into flow visualizations around dynamically scaled physical models of such hairs. To achieve these goals, we needed to compare the flow between hairs moving relative to walls with the flow between them when moving in an unbounded fluid. Since, in practice, we cannot move models through an unbounded fluid in the laboratory, we compared measured flow profiles near physical models of hairs in a tank with those theoretically estimated for such hairs in an unbounded fluid.

Therefore, our physical models had to mimic the geometries and *Re* values for which theoretical flow fields were available. For this reason, our models were pairs of cylinders like those modelled mathematically by Cheer and Koehl (1987*b*), who calculated the fluid flow through pairs of infinitely long cylinders in an unbounded fluid. We simulated 'infinite length' with cylinders that completely spanned one dimension of the experimental tank; thus, although fluid could go around the sides of the array, it could not pass over the ends of the cylinders in the array. This morphology allowed direct comparison with available theoretical predictions in order to estimate the magnitude of wall effects, and thus our physical models differed from the shorter cylinders used by both Leonard (1992) and Hansen and Tiselius (1992). Our physical models represented the biologically relevant *Re* range within which measurable wall effects are anticipated ($Re=10^{-4}$ to 1), and biologically relevant inter-hair spacings (gap:diameter=5:1 and 15:1).

The specific questions addressed by this study were as follows. (1) At what *Re* values does motion relative to walls affect the flow between neighboring hairs? (2) What effect does the distance between a wall and the hairs moving past it have on the flow between the hairs? (3) What effect does the size of the tank in which models are towed have on the flow between the hairs? (4) Does motion parallel to a wall introduce asymmetry in the velocity profile between hairs? (5) Does moving towards a wall have the same consequences for flow between the hairs as moving parallel to a wall? (6) How do walls affect the steepness of velocity gradients near hairs?

The aspect of the flow between neighboring hairs that we measured in this study was leakiness, but we also assessed whether measurements of wall effects on leakiness provided a reasonable indication of wall effects on the steepness of the velocity gradients adjacent to the hairs.

Materials and methods

To assess fluid flow through an array of hairs, scaled-up physical models were towed in a tank of fluid. Small particles acted as fluid markers; their movement relative to the cylinders in the array was recorded photographically and analyzed to estimate leakiness and velocity gradients.

Physical models

We towed cylinders with respect to the walls of a tank to simulate the motion of biological hairs (e.g. sensilla, setules) with respect to nearby stationary surfaces (e.g. body, substratum). Model hairs were constructed of straightened spring steel music wire that was 1.98 or 0.99 mm in diameter (circular cross section) and 400 mm in length (Small Parts Inc., Miami, Florida). Models were towed through a 120 l glass aquarium using a programmable motorized translating table (Daedal single-axis microstepping positioning system MC6023, Western Technology Marketing, Mountain View, CA) (Fig. 2). The cylinders extended to within a few millimeters of the bottom of the towing tank and, hence, essentially spanned the tank to represent 'infinitely long' cylinders, as modeled mathematically by Cheer and Koehl (1987*b*). The cylinders were attached to a towing rod
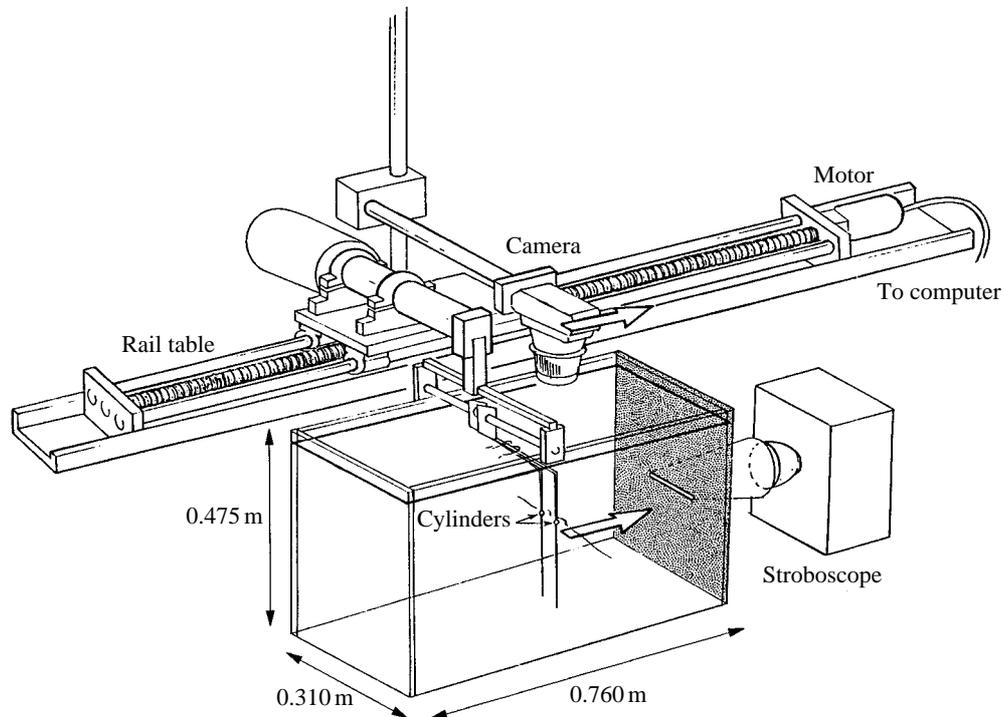
Fig. 2. Experimental apparatus for recording the movement of flow markers past the cylinders. The camera was stationed above, and moved with, the cylinders (movement indicated by arrows). This movement was driven by a motorized rail table controlled by a computer. Flashing light from a stroboscope entered the tank through a horizontal slit.

(the towing rod was above the tank, not in the fluid) and positioned in a vertical orientation (checked with a plumb line). The deflection of the cylinders due to drag as they were towed through the fluid was always less than 2° from vertical; preliminary measurements (using the methods described below) showed that the leakiness of vertically oriented cylinders was indistinguishable from that measured for cylinders inclined 2° from the vertical. The top portion of each cylinder was bent at an angle so that the wires broke through the liquid–air interface at a position 50 mm behind the vertical extension of the cylinders; this was done so that disturbance of the interface did not distort flow visualizations photographed from above the tank. The distance between the cylinders, and that between the cylinders and the side walls, could be adjusted.

Low Reynolds numbers (*Re*) were achieved for our large models by towing them through viscous sugar solutions (which are Newtonian, e.g. Kingsolver and Daniel, 1979). Two fluids were used in the towing tank to allow for the range of *Re* values: full-strength Karo light corn syrup (CPC FoodService, Englewood Cliffs, NJ) for $Re=10^{-4}$, 10^{-3} and 10^{-2}, and dilute Karo syrup (Karo syrup:water 2:1 v/v) for $Re=10^{-1}$ and 1. The average density and viscosity of full-strength Karo syrup at room temperature were 1.37×10^3 kg m^{-3} and 40 Pa s, respectively, and for dilute Karo syrup were 1.26×10^3 kg m^{-3} and 0.04 Pa s. The viscosity of the full-strength Karo syrup was read to
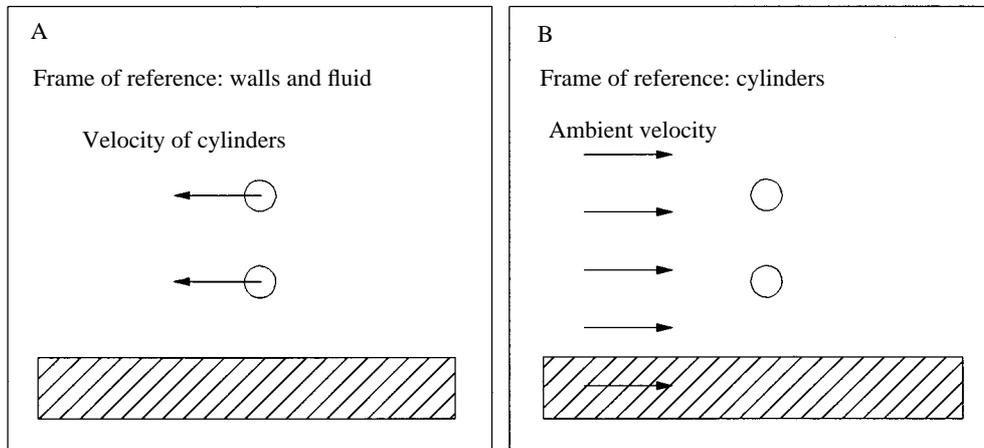
Fig. 3. The flow field relative to a pair of cylinders (observed from the cylinders' frame of reference) will be the same whether the cylinders are moving with respect to stationary surroundings (A) or the surroundings are moving with respect to stationary cylinders (B).

the nearest 0.1 Pa s, and the viscosity of the dilute Karo syrup was read to the nearest 0.002 Pa s using a Rion viscotester (model VT-04, Rion Co. Ltd, Tokyo, Japan). The density of the fluid was estimated by weighing a graduated cylinder containing a known volume of the fluid to the nearest 0.1 mg. The density was measured weekly and did not change appreciably with time. The viscosity of the fluids was sensitive to daily changes in room temperature; therefore, the viscosity of the fluid in the tank was measured on a fluid sample taken from the tank immediately before an experiment was conducted. This measured viscosity was used to calculate the towing velocity required to generate a given *Re*. The temperature was recorded in the room, in the center of the tank and at an edge of the tank, both before and after the towing runs; temperature never varied by more than 1 °C within the tank during a data-collecting session.

Flow visualization

The motion of the fluid relative to the cylinders was indicated by marker particles and recorded by a 35 mm camera that was moved with the cylinders (Fig. 2). Therefore, although the cylinders and camera were moving with respect to the stationary tank of fluid (Fig. 3A), in the frame of reference of the cylinders and photographs, the fluid and the tank walls were moving with respect to the cylinders (Fig. 3B). Hydrogen bubbles were used as flow markers in Karo syrup (Schraub *et al.* 1965; Roos and Willmarth, 1969) while brine shrimp eggs (*Artemia salina*) were used in dilute Karo syrup. The rising rates of the bubbles were less than 0.5 mm s^{-1} and the sinking or rising rates of the eggs were less than 3 mm s^{-1}. The central 10 mm of the cylinders was illuminated through a horizontal slit by a flashing electronic stroboscope (GenRad Strobotac, type 1531, GenRad, Concord, MA). Long-exposure photographs were taken (the exposure was 10–20 times the interval between stroboscope flashes) with a 35 mm camera; thus, the same flow markers were recorded 10–20 times on one exposure as they moved past

the cylinders (Fig. 4A). Preliminary measurements made through the side of the towing tank showed that the flow recorded halfway up the cylinders was representative of the flow experienced by most of the length of the cylinders (the central 0.360 m of 0.400 m). The cylinders had reached a constant velocity and had moved 0.010–0.020 m before a photograph was taken. During the exposure, the cylinders moved a total distance of 0.02–0.10 m.
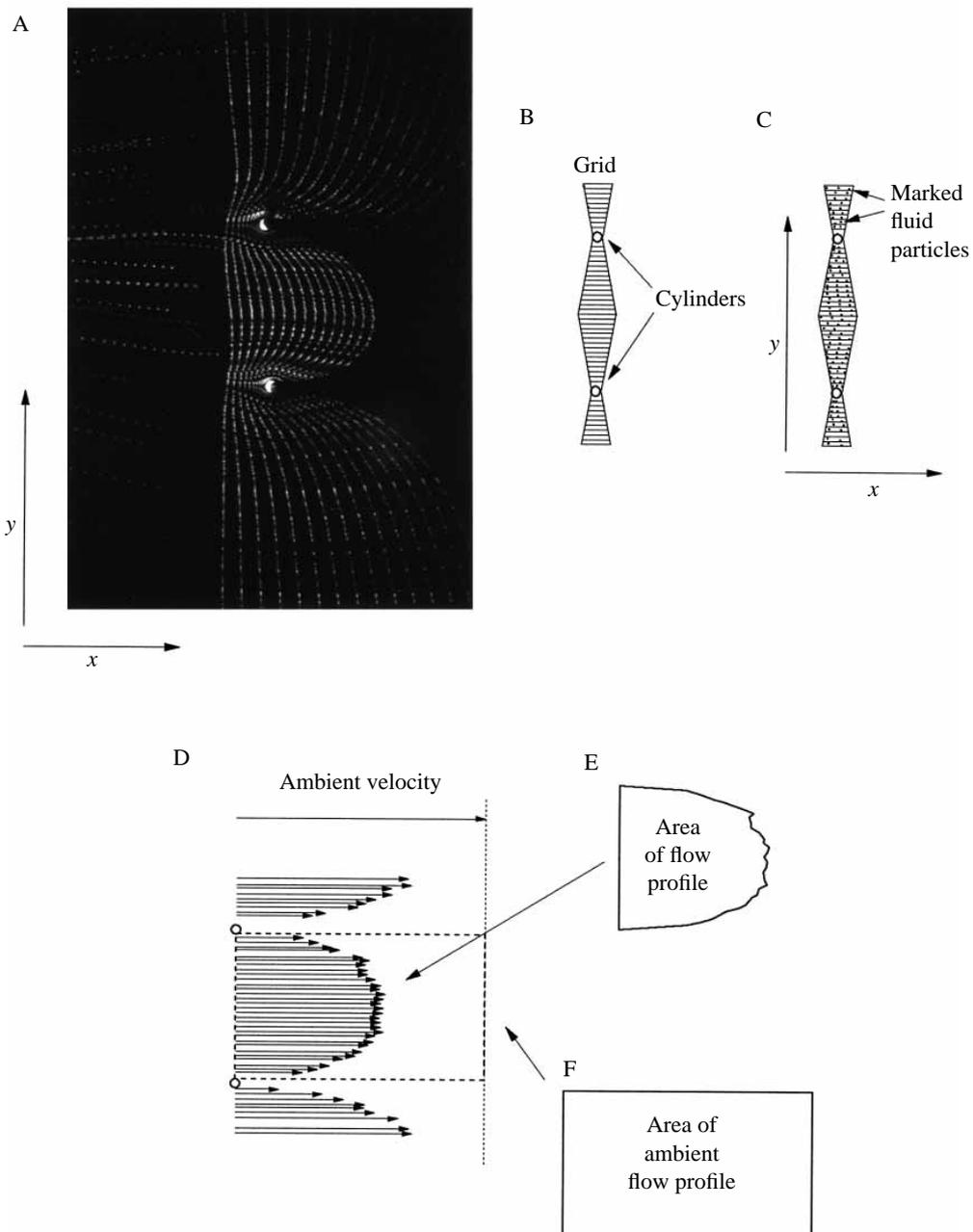

Fig. 4

Experimental manipulations

To test the effects of nearby walls on the flow between cylinders with different spacings operating at a variety of *Re* values, we varied the geometry, speed and fluid in our towing tank to produce the following experimental treatments: five *Re* values (10^{-4}, 10^{-3}, 10^{-2}, 10^{-1} and 1), two gap:diameter ratios (15:1 and 5:1) and up to six positions relative to the walls (described in Results). The actual gap:diameter ratio and distance to the walls for each experiment were measured from photographs. Both gaps and distances to walls were measured from the nearest edges, not the centers, of the cylinders. The average measured gaps for the 15:1 and 5:1 gap:diameter ratio treatments (in cylinder diameters ±1 standard deviation) were 15.2±0.4 (*N*=119) and 5.2±0.6 (*N*=92) respectively. The distances measured from the closest side wall were usually within 1 cylinder diameter and always within 2 cylinder diameters of the desired distance.

Three replicates were made for most experimental treatments; only one replicate was made for the lowest *Re* (10^{-4}), and up to five replicates were made for *Re*=10^{-1} because of the greater experimental variance in the latter. The greater variance at *Re*=10^{-1} is a consequence of the relatively greater magnitude of the random movements of the marker particles in the dilute Karo solution at the slow towing speeds required for this *Re*, and is not due to the unsteady phenomena documented by Leonard (1992). A 'replicate' was a data set generated for a single pair of cylinders towed through the tank for a given combination of *Re*, gap:diameter ratio and position in the towing tank. Each replicate for a particular *Re*, gap:diameter ratio and position used different cylinders and was usually taken on a different day using different fluid in the tank.

Flow analysis

Leakiness was measured as described in Fig. 4. Sometimes no particle travelled through a spatial interval and hence no velocity estimate could be made for that interval. We eliminated a replicate if fewer than 80 % of the spatial intervals contained velocity estimates. A leakiness estimate based on 80 % of the intervals was within 5 % of the

---

Fig. 4. Technique for measuring leakiness. A photograph (A) of a single line of flow markers (hydrogen bubbles) moving past a pair of cylinders was taken with the camera attached to the apparatus shown in Fig. 2. The single line appears as a series of lines because the shutter of the camera was left open much longer than the time interval between stroboscope flashes. The cylinders appear as circles because they are viewed along their longitudinal axes. In order to calculate the velocities in each spatial interval, a photograph (A) was projected onto a grid (B) and single flow markers were traced onto the grid (C). The magnitude of the velocity was determined by dividing the distance traversed by a single flow marker in a known amount of time corresponding to two or more stroboscope flashes. The position of the velocity vector (the *y* coordinate) was estimated from the *y* coordinate of the particle closest to the line connecting the centers of the two cylinders (except for the spatial intervals immediately adjacent to the cylinders, where the *y* coordinate was estimated from the intersection of the circular path of the particle with the line connecting the centers of the two cylinders). The calculated velocites were used to construct a velocity profile (D). Leakiness was estimated from the ratio of the area of the polygon formed by the velocity estimates (assuming zero velocity at the edges of the cylinders) (E) to the area of the rectangle formed by the ambient velocity and the gap between the cylinders (F).

leakiness estimate based on 100 % of the intervals (comparing leakiness calculated for 20 complete data sets and recalculated for the same data sets after discarding 20 % of the intervals; the discarded intervals were those immediately adjacent to the cylinders because these intervals were the most likely to be missing fluid markers).

Results

At which Re *values does motion relative to the walls affect the flow between neighboring hairs?*

The consequences of stationary walls to the flow between cylinders moving past them depends on the Reynolds number (Fig. 5). At an *Re* of 1, the leakinesses measured for cylinders moving relative to walls were not significantly greater than the theoretical predictions for cylinders moving in an unbounded fluid, indicating that wall effects were negligible for the range of variables we measured (i.e. *P*>0.05 for all twelve one-tailed *t*-test comparisons of the data for all gap:diameter ratio and wall distance combinations at *Re*=1 with the theoretical value available for *Re*=0.5). Similarly, no wall effects were

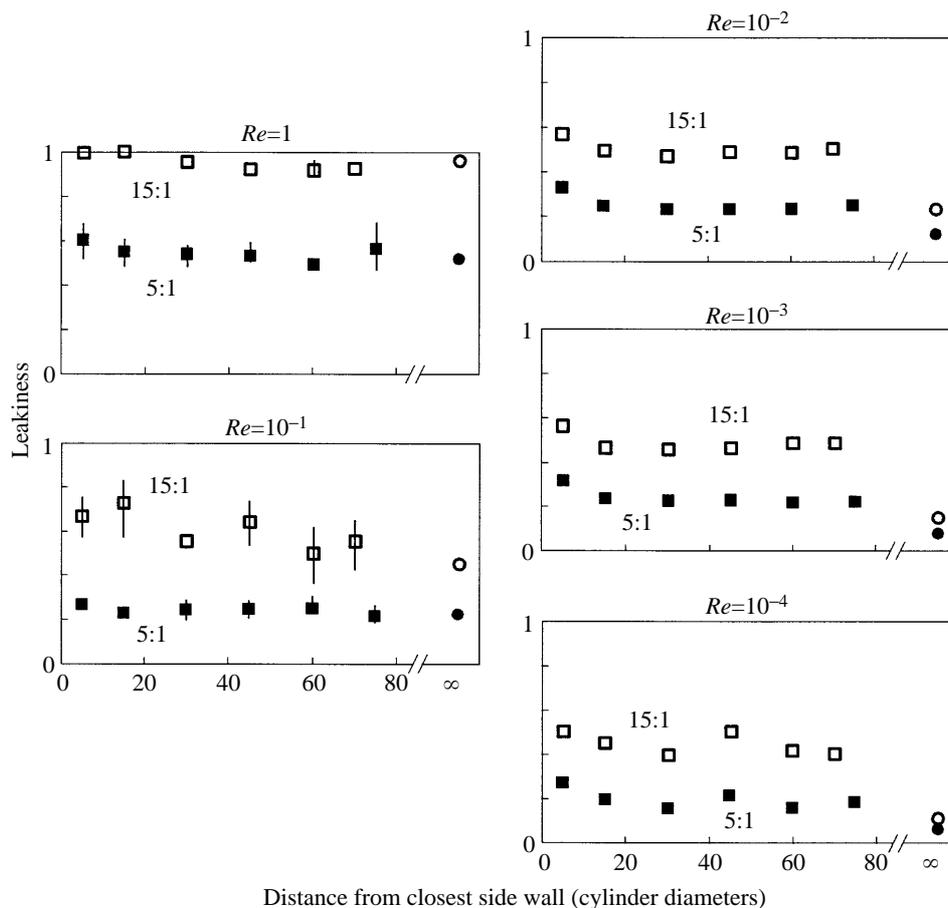Distance from closest side wall (cylinder diameters)

Fig. 5

observed for closely spaced cylinders (gap:diameter ratio of 5:1) at an Re of 10^{-1}. In contrast, leakiness was roughly 30 % greater than the theoretical predictions for widely spaced cylinders (15:1) at this Re. Wall effects were more dramatic at Re values of 10^{-2} and below, where movement relative to a wall increased leakiness by a factor of 2–3. Since Re is a function of both the diameter and the speed of cylinders (equation 1), our results indicate that the arrays of hairs most sensitive to wall effects are those moving very slowly and those composed of very fine hairs.

What effect does the distance between a wall and the hairs moving past it have on the flow between the hairs?

Changing the distance between the nearest wall and the cylinders moving past it had little effect on leakiness, except when the cylinders were very close to the wall (Fig. 5). At Re values of 10^{-2} and below, leakiness was higher when hairs moved parallel to walls that were only 5 diameters away than when the walls were more distant.

Our observation that the magnitude of the wall effect changed very little with distance from the nearest wall could simply have been an artifact of conducting the experiments in a tank; positioning the cylinders farther from one wall necessitated placing them closer to the opposite wall of the tank. However, when we calculated how the skin friction drag on a cylinder varied with distance from a *single* wall (Happel and Brenner, 1965; Tritton, 1988), we found a similar relationship to that measured for leakiness (compare Figs 5 and 6). (Since both skin friction drag and leakiness increase with the steepness of the velocity gradient at the surface of the cylinders, we would expect them to vary in a similar way with flow profile.) Although this suggested that the insensitivity of leakiness to distance from the nearest wall was not simply a tank artifact, we felt it was important to assess the effects of tank size on leakiness.

What effect does the size of the tank in which models are towed have on the flow between the hairs?

In an empirical study where it is not possible to have only a single wall, the relative

Fig. 5. Mean leakiness (range indicated by error bars) of a pair of cylinders as a function of their distance from the closest wall parallel to which they were moving. The leakiness predictions for walls infinitely far away from a wall (circles) are from Cheer and Koehl (1987*b*). The theoretical predictions plotted for $Re=1$ are actually the values calculated for $Re=0.5$, since no theoretical prediction is available for $Re=1$. When $Re \leqslant 10^{-2}$, leakiness was significantly greater when the cylinders moved very close to the wall (5 cylinder diameters) than when they moved farther away (15 diameters) (for $Re \leqslant 10^{-2}$ there are six different Re/gap size combinations for which the two wall distances can be compared; analyzing each Re/gap size combination separately results in $P<0.05$ for each ANOVA of leakiness for every combination with a sufficient sample size for statistical testing; identical results were obtained with non-parametric testing using the Mann–Whitney U-test). However, leakiness decreased very slowly with distance from the wall when that distance was $\geqslant 15$ cylinder diameters at $Re \leqslant 10^{-2}$, and when that distance was $\geqslant 5$ cylinder diameters when $Re=1$ and 10^{-1}. Excluding the closest distance to the wall (5 cylinder diameters), only 2 out of the 10 groups of data showed a significant downward trend in leakiness with increasing distance from the wall: the 15:1 gap:diameter ratio for $Re=1$ and the 15:1 gap:diameter ratio for $Re=10^{-1}$ (all other slopes calculated by linear regression were not significantly less than zero, $P>0.05$).
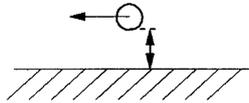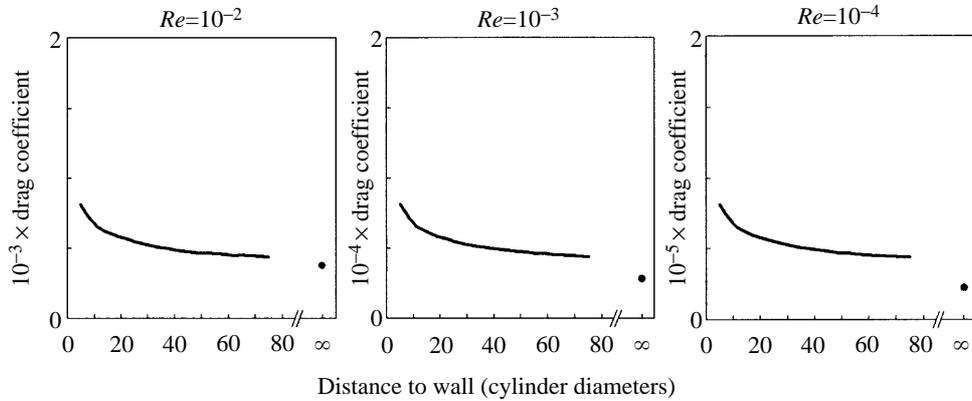
Fig. 6. The drag coefficient (dimensionless) of a single cylinder in the presence of a single wall was predicted to change rapidly with distance very close to the wall and then to decrease only very slowly as the cylinder moved farther and farther away from the wall. The abscissa shows the same values in Figs 5 and 6 to facilitate visual comparison. Motion was parallel to the wall, as indicated. The viscosity and density of the fluid were the same as those of Karo syrup and the diameter of the cylinder was 1.98 mm. Drag in the presence of a single wall was calculated from Takaisi's equation (Happel and Brenner, 1965: equation 7-7.25, p. 346), and drag in the absence of walls was calculated from Lamb's equation (Tritton, 1988: equation 9.19, p. 112). Happel and Brenner (1965) defined distance to the wall from the center of the cylinder; here, distance to the wall means distance from the closest edge of the cylinder consistent with Cheer and Koehl (1987b).

effects of the closest wall compared with those of the other walls may be evaluated by keeping the distance to one wall constant while increasing the distances to the other walls. This could be achieved by enlarging the experimental tank, but a simpler approach is to use cylinders of smaller diameter, to move them more rapidly so as to keep Re the same as for the thicker cylinders, and to keep their distance (in cylinder diameters) from the nearest wall the same. Although we used the latter approach, we shall refer to this manipulation as 'enlarging the tank,' since it is functionally the same.

Fig. 7 illustrates the consequences to leakiness of enlarging the tank in which the models were towed. When the cylinders were extremely close to the nearest wall, the leakiness values for the two tanks converged, indicating that the influence of the nearest wall overshadowed that of the other boundaries in the tank. However, at all the distances we tested of 15 cylinder diameters or more from the closest wall, hairs in the larger tank were significantly less leaky than those in the smaller tank, indicating that tank walls other than the one nearest to the model did indeed contribute to increasing the leakiness of the hairs. Leakiness more closely approached the theoretical (no walls) value when the tank was effectively bigger, which is further evidence suggesting that wall effects are
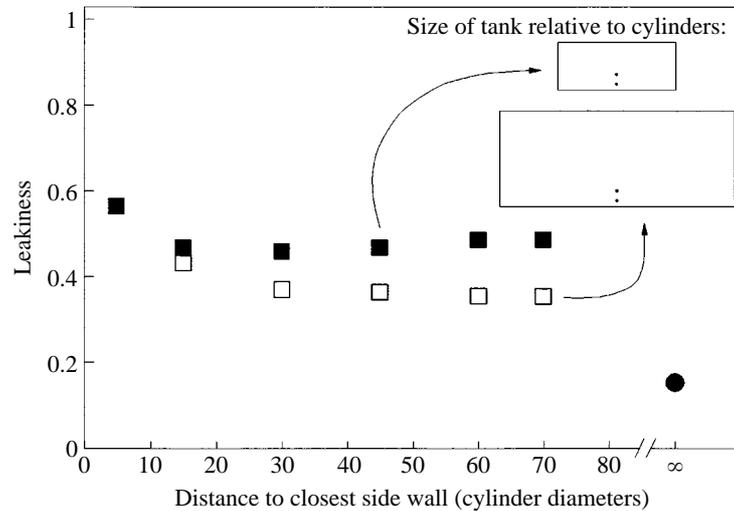
Fig. 7. Leakiness values for a 'larger' tank (open squares) were closer to the theoretical 'no walls' predictions than leakiness values measured in a 'smaller' tank (filled squares) for $Re=10^{-3}$. Means of replicates are plotted; in all cases, the complete range of replicates falls within the size of the symbol. The size and spacing of the cylinders are greatly exaggerated relative to the size of the tank to make them visible. Fifteen diameters was the closest possible distance for the 'larger' tank.

responsible for the deviation of empirical measurements from theoretical predictions of leakiness.

Does motion parallel to a wall introduce asymmetry in the velocity profile between hairs?

How much asymmetry is introduced into the velocity profile between hairs moving parallel to a wall if one hair is closer to the wall than the other? One way of testing for asymmetry of the flow through the gap between the hairs is to compare the leakiness of one half of the gap with the leakiness of the other half (Fig. 8). We found no significant differences between the leakinesses of the two halves of a gap, except when the more widely spaced cylinders (15:1) were very close to the wall (5 diameters) at *Re* values less than 1. Even in these cases, the half of the gap closer to the wall was only about 15 % leakier than the other half of the gap. As illustrated in Fig. 9A, when cylinders were very close to a wall, although velocity profiles were only slightly asymmetrical between the hairs, velocities could be considerably faster in the space between the wall and the adjacent hair than around the edge of the array that was farther from the wall.

Does moving towards a wall have the same consequences for flow between the hairs as moving parallel to a wall?

A hair-bearing appendage may move parallel or perpendicular to a wall. As was the case with motion parallel to the nearest wall, the leakiness of a pair of cylinders was insensitive to their distance from the wall towards which they were moving until they came close (15 diameters) to the wall (Fig. 10).
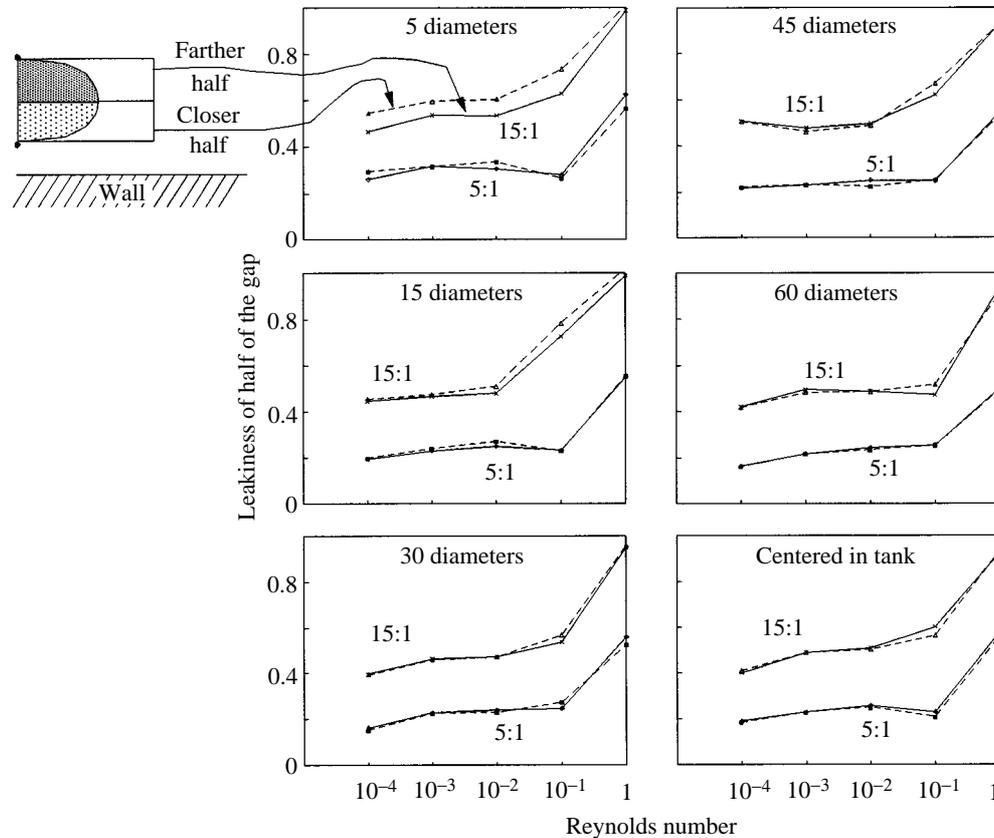
Fig. 8. Velocity profiles were tested for asymmetry by comparing leakiness of the two halves of the gap. In each case, the dashed line represents the leakiness of the half closer to the wall and the solid line the leakiness of the half farther from the wall. Each individual graph is for one distance (given in cylinder diameters) relative to the closest side wall (motion was parallel to the closest wall). The only examples in which the leakinesses of the two halves were significantly different (indicating asymmetry in the velocity profile) were for the cylinders with a gap:diameter ratio of 15:1 at $Re<1$ when the cylinders were 5 cylinder diameters from the wall (top left-hand graph in figure) ($P<0.05$ for one-tailed t-tests for each Re: $Re=10^{-3}$, 10^{-2}, 10^{-1}). No statistical tests are possible for $Re=10^{-4}$ because the sample sizes were only $N=1$.

How do walls affect the steepness of velocity gradients near hairs?

As described in the Introduction, both the leakiness of an array of hairs and the steepness of the velocity gradients next to the hairs affect their performance in capturing molecules or particles. Although we shall discuss elsewhere (B. A. Best, C. Loudon and M. A. R. Koehl, in preparation) the effects of array morphology on the velocity gradients near hairs, we thought it useful to address here the relationship between wall effects on leakiness and wall effects on velocity gradients.

Examples of velocity profiles (at $Re=10^{-3}$) measured between cylinders moving near a wall and calculated between cylinders in an unbounded fluid are shown in Fig. 9A. If
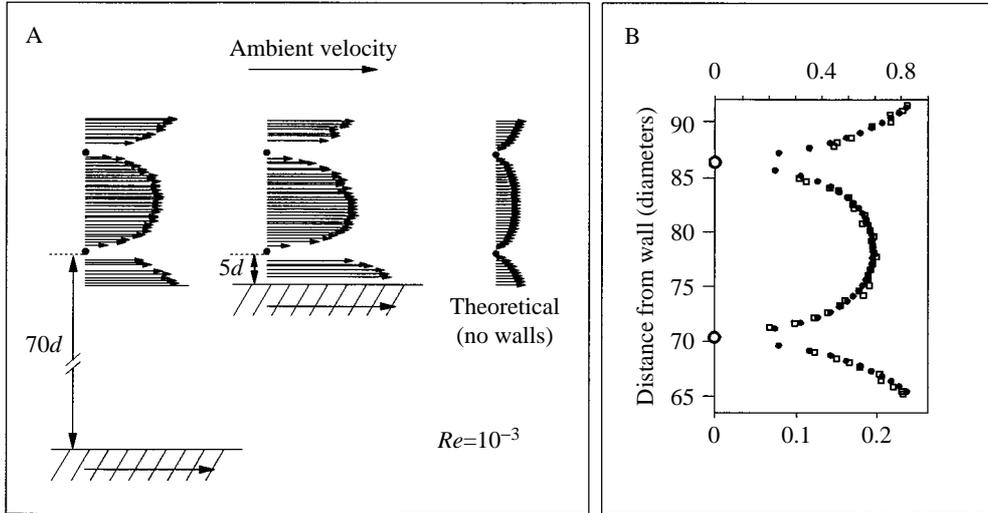
Fig. 9. (A) Leakiness in the presence of a wall was approximately three times greater than theoretically predicted both when the closest wall was only 5 cylinder diameters (5*d*) away and when it was 70 diameters (70*d*) away for *Re*=10^{-3} (theoretical velocity profile is from A. Y. L. Cheer and M. A. R. Koehl, unpublished results). (B) The theoretical velocity profile (●, bottom) and the empirical velocity profile (□, top) 70 cylinder diameters from the closest wall (both from A and normalized to ambient velocity) are plotted together using different scales to demonstrate that the shapes of the two curves are virtually identical (i.e. the ratio of velocities at any two corresponding points are the same in the two curves).

we normalize the vectors in each case by dividing them by the peak velocity reached between the cylinders, we find that the velocity profile between cylinders at the center of the tank and between those in an unbounded fluid are nearly identical (Fig. 9B). Hence, when motion near a wall increases the leakiness between hairs by a given factor, each velocity vector between the hairs is increased by that factor. For these cases where the velocity profile is uniformly changed, the relationship between leakiness and velocity gradients near the hairs is very simple: for a given morphology, leakiness is changed by the same factor as velocity gradient. A single number can be calculated to represent the shape of a velocity profile between hairs: the coefficient of variation of the *N* position coordinates of the velocity vectors (y_i), each weighted by the magnitude of its velocity (v_i), provides a description of the distribution of velocities about the midpoint of the gap:

$$\text{velocity distribution index} = \frac{\sqrt{\{\Sigma[v_i(y_i-\bar{y})^2]/(N-1)\}}}{\bar{y}}, \tag{3}$$

where

$$\bar{y} = (\Sigma v_i y_i)/(\Sigma v_i). \tag{4}$$

Thus, this velocity distribution index is directly analogous to the coefficient of variation used to describe the distribution of values about a mean (Sokal and Rohlf, 1981). Unlike
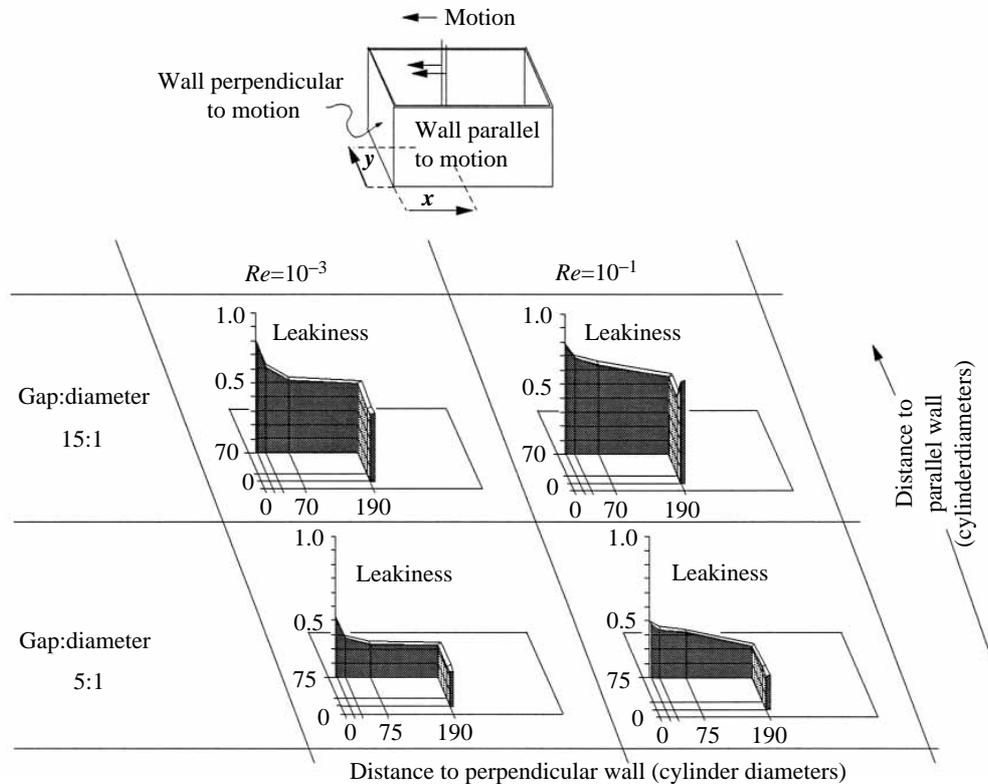
Fig. 10. Leakiness (z axis, vertical) as a function of position in experimental tank; the distances to all four walls are indicated by the position relative to the four sides of the x,y rectangle.

the test performed above, which evaluated asymmetry by comparing the two halves of a gap, this index describes the spread of velocities about the middle; the higher the index, the steeper the velocity gradient will be near the hairs for the same value of velocity in the middle. This velocity distribution index was not affected by Re or distance from the wall ($P>0.05$ for Re and distance to closest wall in an analysis of variance of velocity distribution index; only symmetrical profiles were tested). Therefore, this means that, for a given morphology in low-Re flow ($Re\leqslant1$), a change in leakiness (which is easy to measure) implies a comparable change in velocity gradients near the hairs (which is quite difficult to measure).

Discussion

Biological consequences of wall effects on flow between hairs

Animals from a number of phyla use appendages bearing arrays of hairs to perform a variety of important functions. Because fluid can move around or through a group of hairs, the leakiness of the array of hairs on an appendage can affect its performance at filtering substances from the surrounding fluid or at propelling the fluid. Many animals

move their hair-bearing appendages relative to their bodies and to surfaces in their environments; hence, the effects of walls on flow through the hairs must be considered when the function of appendages is analyzed.

Consequences of size or speed

Our results indicate that if an animal moves an appendage bearing a row of hairs along or towards a nearby stationary wall, the effects of that wall on the flow between the hairs depends on Reynolds number, i.e. on the diameters and speeds of the hairs (equation 1).

$Re \leqslant 10^{-2}$. When Re is 10^{-2} or lower, moving relative to a wall increases the leakiness of the array of hairs (by a factor of 2–3) and produces steeper velocity gradients next to the hairs. Closely spaced hairs are less sensitive to these wall effects than are hairs with wide gaps between them. Furthermore, in this very low Re range, gap width has a large effect on leakiness *if* the appendage moves with respect to a wall, but *not* if it moves in an unbounded fluid. Hence, at these very low Re values, a morphological feature with little consequence in an unbounded fluid can acquire a pronounced effect on performance if the appendage moves near a wall.

$10^{-1} \leqslant Re \leqslant 1$. At an Re of 1, the fluid flow between neighboring hairs is unchanged by motion near a wall. At an Re of 10^{-1}, walls also have no noticeable effect on the leakiness of closely spaced cylinders and increase leakiness only slightly for widely spaced hairs. At Re values of 10^{-1} to 1, an increase in the width of the gap between hairs raises leakiness whether walls are present or not.

Thus, there is a transition within the low-Re realm where the 'rules of the game' change for arrays of hairs as predicted theoretically by Cheer and Koehl (1987*a,b*). If the size of the hairs in an array increases during the growth of an individual or the evolution of a lineage, such that hair Re rises from below 10^{-2} towards 1, then the following changes take place: (1) arrays that functioned like paddles at very low Re become leakier and can act as filters; (2) motion relative to walls no longer increases the leakiness of the array, and (3) the proportion of fluid moving through, rather than around, an array becomes sensitive to the speed at which the array moves. Therefore, the consequences of morphological or behavioral differences between organisms are different at very low ($Re \leqslant 10^{-2}$) and at moderately low Re values ($10^{-1} \leqslant Re \leqslant 1$).

Calanoid copepods provide an example of the Re-dependence of wall effects on the leakiness of a hair-bearing appendage. These small planktonic crustaceans capture food particles by flapping setulose appendages, the second maxillae (Fig. 1C). Leakiness was measured at 0.9 between the setae (hairs) of the second maxillae of one species of copepod, *Centropages furcatus*, which operates its second maxillae at $Re \approx 1$ (based on seta diameter), where wall effects are less important; this measurement shows good agreement with the corresponding theoretical 'no walls' prediction of 0.9 (Koehl, 1992). In contrast, a leakiness of 0.2 was measured for the second maxillae of a different species of copepod, *Eucalanus pileatus*, which operates its second maxillae at $Re \approx 10^{-2}$; this measurement is *twice* the value of 0.1 predicted theoretically in the absence of walls (Koehl, 1992). Because copepods flap their second maxillae with respect to their bodies and each other, we suggest that wall effects are responsible for the deviation of the measured leakiness from the theoretical predictions for the low-Re species.

Behavior patterns that alter leakiness

This study suggests that the methods an organism can use to alter the leakiness of a hair-bearing appendage differ with *Re*. When *Re* is between 10^{-2} and 1, changes in speed have a big effect on leakiness, while movement near walls makes little difference. In contrast, when $Re \leqslant 10^{-2}$, changing speed does not alter leakiness, whereas movement relative to a wall increases it. Although, at these very low *Re* values, wall effects are felt at distances of many diameters from the surface, an organism can change its leakiness by altering appendage distance from the wall only when the appendage is very near to the wall. At distances greater than about 10 or 15 diameters from the wall, there is considerable scope for changes in appendage distance from the wall without consequent changes in leakiness. Note that, although changing the speed of appendage motion at very low *Re* values does not alter the proportion of the fluid that moves through, rather than around, an array of hairs, it does change the velocity of fluid motion through the appendage and, hence, the absolute volume per time processed (the difference between leakiness and velocity gradient is further discussed in B. A. Best, C. Loudon and M. A. R. Koehl, in preparation).

Hinged appendages

Many hair-bearing appendages are hinged and flap with respect to the surface of an animal's body. The tip of a hinged appendage moving at a given angular velocity moves at a greater speed (higher *Re*) than the proximal end of the appendage; hence, we would expect leakiness to vary along the length of such an appendage if the tip were to operate at *Re* values of 10^{-1} to 1. Does the proximity of the body wall help to compensate for this reduced leakiness near the base of the appendage? The motion of the physical models in this study was non-rotational, but the leakiness estimates made as a function of *Re* and wall distance can be used to make an approximation of the flow through hairs at different distances from the hinge. As illustrated by the examples in Fig. 11, although wall effects can increase the leakiness of the proximal end of a hinged appendage to approximate more closely the leakiness of more distal parts, the velocity of fluid motion near the tips still remains much higher. Therefore, for filter-feeding appendages, gills or olfactory antennae undergoing hinged motion, the distal end of the structure processes most of the fluid.

Distances at which wall effects are important

If we rearrange equation 2 to eliminate *L*, we can estimate the distance (*Y*) beyond which a wall should have no effect on the flow around an object moving with respect to the wall at velocity *U*:

$$Y > 20\nu/U, \tag{5}$$

where ν is the kinematic viscosity of the fluid ($15 \times 10^{-6} \, \text{m}^2 \, \text{s}^{-1}$ for air and $1 \times 10^{-6} \, \text{m}^2 \, \text{s}^{-1}$ for water, both at 20 °C; Vogel, 1981). [Note that this estimate of *Y* is conservative (Vogel, 1981), as equation 2 was derived by White (1946) from the intersection of the equation fitted to his empirical measurements on drag on single
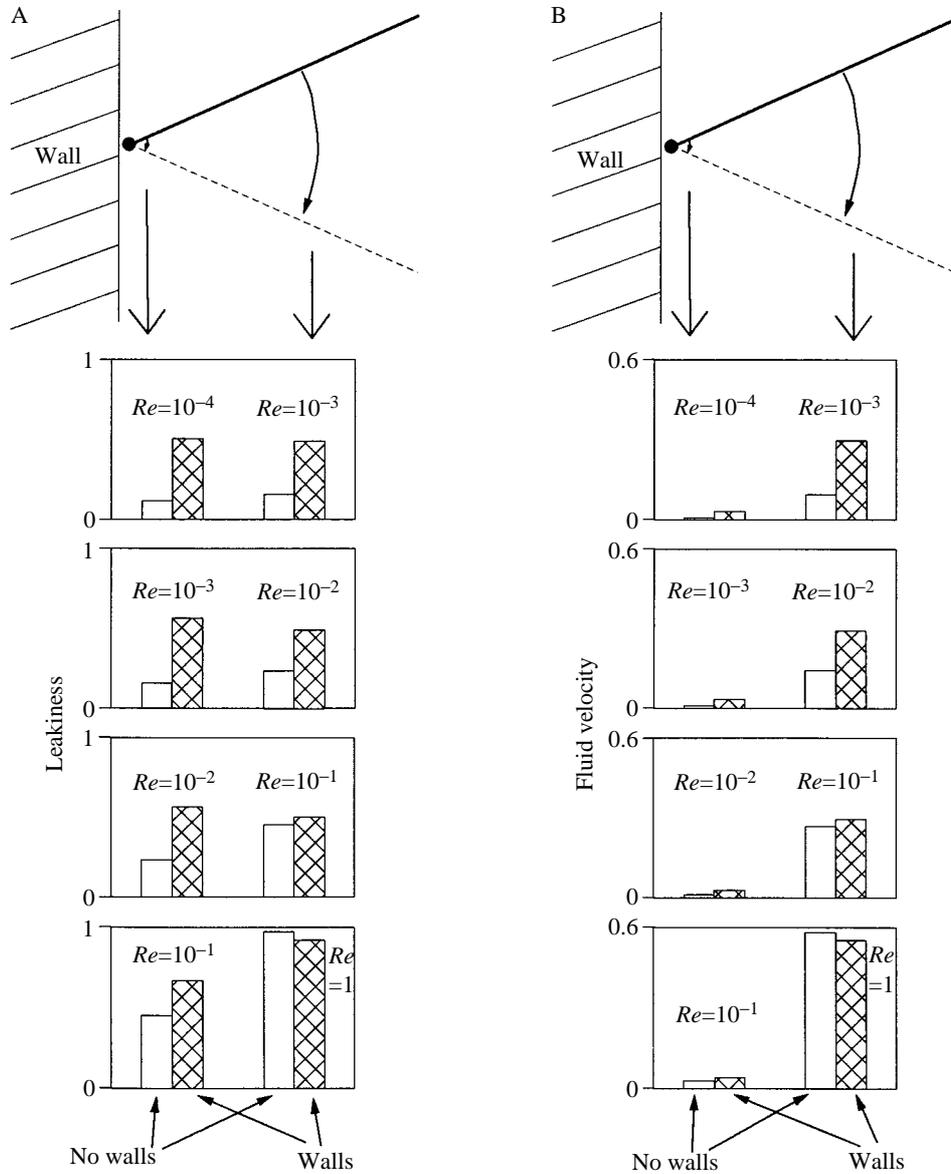
Fig. 11. The tip of a hinged appendage moves more rapidly than the base; thus, the Reynolds number varies along the length of the appendage. Two points on the appendage, located 6 and 60 units from the hinge of a 100 unit appendage, were selected for discussion purposes. (A) The presence of a wall tended to lessen the differences in leakiness along the appendage (hatched bars) predicted in the absence of wall effects (open bars; values from Cheer and Koehl, 1987*b*). (B) However, the average fluid velocity passing between two hairs was much greater farther from the hinge; thus, more fluid is processed by more distal parts of a hinged appendage undergoing rotational motion about its hinge. Values plotted are the average fluid velocity between two hairs divided by the velocity of the tip of the appendage as it moves through the fluid.

cylinders in the presence of walls with the theoretical equation predicting drag in the absence of walls. For estimating a less conservative distance, such as the distance at which wall effects increase drag by only 5 % over the theoretical value, the 20 in equations 1 and 2 should be replaced by 10 or 15, depending on Re.] For an object moving in air at $1\,\mathrm{m\,s}^{-1}$, wall effects are negligible when $Y>300\,\mu$m, whereas for a slower body moving at only $0.1\,\mathrm{m\,s}^{-1}$, wall effects cannot be ignored until $Y>3$ mm. Wall effects are not felt at such large distances in water: for an object moving at $0.1\,\mathrm{m\,s}^{-1}$, wall effects are negligible when $Y>200\,\mu$m, and for a body going only $0.01\,\mathrm{m\,s}^{-1}$, $Y>2$ mm. Thus, although wall effects at low Re values are felt by a body at great distances from a surface *if distance is measured in body diameters*, the absolute distances (measured in millimeters) from the wall at which the effects are noticeable are quite small. This consideration, together with the very low Re values at which wall effects are important, suggests that we need only worry about the consequences to leakiness of moving relative to walls for very tiny creatures or appendages. Another factor that can modify the distance at which wall effects are felt by a very small body is the propulsion of fluid at the surface of that body, such as that caused by the beating of cilia; for example, the wall effects experienced by a ciliated protozoan at about 3 body diameters from a wall when the cilia are beating are comparable to those experienced by a protozoan with motionless cilia at about 60 body diameters from the wall (Winet, 1973).

Effects of the tank on flow near physical models at low Reynolds number

Our results also have important implications for modelling studies of bodies operating at very low Re, where flow can be affected by walls that are hundreds of diameters away. The use of mathematical models or of dynamically scaled large physical models of small structures permits us to assess details of the fluid motion that would be technically very difficult to measure for the real biological appendages. For example, our measurements of velocity at intervals of 1 cylinder radius correspond to measurements at intervals of $1\,\mu$m relative to a sensillum $2\,\mu$m in diameter on a moth antenna. Unfortunately, we found that the size of the tank through which a dynamically scaled physical model is towed affects its leakiness at $Re=10^{-3}$, although models at Re values of 10^{-1} and above can be operated without wall effects. However, since many hair-bearing appendages operate near boundaries in the habitat as well as near the body of the animal, measurements made using models towed in tanks may provide a more realistic view of the flow than would mathematical models in unbounded fluids.

Except for the region immediately adjacent to a wall, leakiness changes only very slowly with distance from the wall. A common procedure for assessing wall artifacts in a tank is to make a measurement on the test object at increasing distances from the tank wall until no change in value with distance from the wall is recorded. Our results point out the danger of this approach for objects with a very low Re value: after an initially rapid decrease in leakiness with distance from the wall, leakiness appears to be independent of further changes in distance, although, in fact, it is still greatly increased by the wall. The small slope of leakiness as a function of distance does not indicate that the wall effect is negligible, but rather that the magnitude of the wall effect is not changing very rapidly with distance.

Therefore, although physical models towed in tanks are useful for studying organisms or appendages that operate near surfaces in nature, they introduce artifacts for those that move far from any wall. However, because of the relationship between leakiness and velocity profile that we described (the velocity profile changes uniformly by the same factor as leakiness in the presence of a wall), it may be possible in the future to develop methods to correct mathematically for such 'tank wall effects'. Conversely, mathematical models of structures with very low *Re* values will misrepresent the flow and forces for organisms that move near walls unless stationary boundaries are incorporated into the calculations.

References

ADAM, G. AND DELBRÜCK, M. (1968). Reduction in dimensionality in biological diffusion processes. In *Structural Chemistry and Molecular Biology* (ed. A. Rich and N. Davidson), pp. 198–215. San Francisco: W. H. Freeman.

ALTNER, H. AND PRILLINGER, L. (1980). Ultrastructure of invertebrate chemo-, thermo- and hygroreceptors and its functional significance. *Int. Rev. Cytol.* **67**, 69–139.

CHEER, A. Y. L. AND KOEHL, M. A. R. (1987*a*). Fluid flow through filtering appendages of insects. *IMA J. appl. Math.* **4**, 185–199.

CHEER, A. Y. L. AND KOEHL, M. A. R. (1987*b*). Paddles and rakes: fluid flow through bristled appendages of small organisms. *J. theor. Biol.* **129**, 17–39.

DeSIMONE, J. A. (1981). Physicochemical principles in taste and olfaction. In *Biochemistry of Taste and Olfaction* (ed. R. H. Cagan and M. R. Kane), pp. 213–229. New York: Academic Press.

FUTRELLE, R. P. (1984). How molecules get to their detectors; the physics of diffusion of insect pheromones. *Trends Neurosci.* **7**, 116–120.

GHIRADELLA, H. T., CASE, J. F. AND CRONSHAW, J. (1968). Structure of aesthetascs in selected marine and terrestrial decapods: chemoreceptor morphology and environment. *Am. Zool.* **8**, 603–621.

GIBSON, G. AND BRADY, J. (1985). 'Anemotactic' flight paths of tsetse flies in relation to host odour: a preliminary video study in nature to loss of odour. *Physiol. Ent.* **10**, 395–406.

HANSEN, B. AND TISELIUS, P. (1992). Flow through the feeding structures of suspension feeding zooplankton: a physical model approach. *J. Plankton Res.* **14**, 821–834.

HAPPEL, J. AND BRENNER, H. (1965). *Low Reynolds Number Hydrodynamics with Special Applications to Particulate Media.* Englewood Cliffs: Prentice-Hall, Inc.

JØRGENSEN, C. B. (1983). Fluid mechanical aspects of suspension feeding. *Mar. Ecol. Prog. Ser.* **11**, 89–103.

KINGSOLVER, J. G. AND DANIEL, T. L. (1979). On the mechanics and energetics of nectar feeding in butterflies. *J. theor. Biol.* **76**, 167–179.

KOEHL, M. A. R. (1992). Hairy little legs: feeding, smelling and swimming at low Reynolds number. In *Fluid Dynamics in Biology: Proceedings of an AMS-IMS-SIAM Joint Research Conference* (ed. A. Y. Cheer and C. P. van Dam). *Contemporary Mathematics* **141**, 33–64. Providence: American Mathematical Society.

LABARBERA, M. (1984). Feeding currents and particle capture mechanisms in suspension feeding animals. *Am. Zool.* **24**, 71–84.

LEONARD, A. B. P. (1992). The biomechanics, autecology and behavior of suspension-feeding in crinoid echinoderms. PhD dissertation, University of California, San Diego.

MOORE, P. A., ATEMA, J. AND GERHARDT, G. A. (1991). Fluid dynamics and microscale chemical movement in the chemosensory appendages of the lobster, *Homarus americanus. Chem. Sens.* **16**, 663–674.

MURRAY, J. D. (1977). Reduction of dimensionality in diffusion processes: antenna receptors of moths. In *Lectures on Nonlinear-Differential-Equation Models in Biology*, pp. 83–127. Oxford: Oxford University Press.

ROOS, F. W. AND WILLMARTH, W. W. (1969). Hydrogen bubble flow visualization at low Reynolds numbers. *AIAA J.* **7**, 1635–1637.

RUBENSTEIN, D. I. AND KOEHL, M. A. R. (1977). The mechanisms of filter feeding: some theoretical considerations. *Am. Nat.* **111**, 981–994.

SCHRAUB, F. A., KLINE, J., HENRY, J., RUNSTADLER JR, P. W. AND LITTELL, A. (1965). Use of hydrogen bubbles for quantitative determination of time-dependent velocity fields in low-speed water flows. *J. basic Eng. Trans. ASME Ser. D* **June**, 429–444.

SHIMETA, J. AND JUMARS, P. A. (1991). Physical mechanisms and rates of particle capture by suspension-feeders. *Oceanogr. mar. Biol. A. Rev.* **29**, 191–257.

SOKAL, R. R. AND ROHLF, F. J. (1981). *Biometry; The Principles and Practice of Statistics in Biological Research.* Second edition. New York: W. H. Freeman and Co.

SPIELMAN, L. AND GOREN, S. L. (1977). Model for predicting pressure drop and filtration efficiency in fibrous media. *Env. Sci. Technol.* **2**, 279–287.

SRYGLEY, R. B. AND DUDLEY, R. (1993). Correlations of the position of center of body mass with butterfly escape tactics. *J. exp. Biol.* **174**, 155–166.

STEINBRECHT, R. A. (1970). Zur Morphometrie der Antenne des Seidenspinners, *Bombyx mori* L.: Zahl und Verteilung der Riechsensillen (Insecta, Lepidoptera). *Z. Morph. Tiere* **68**, 93–126.

TRITTON, D. J. (1988). *Physical Fluid Dynamics.* Oxford: Oxford University Press.

VOGEL, S. (1981). *Life in Moving Fluids; the Physical Biology of Flow.* Boston: Willard Grant Press.

WHITE, C. M. (1946). The drag of cylinders in fluids at slow speeds. *Proc. R. Soc. A* **186**, 472–479.

WILLIS, M. A. AND ARBAS, E. A. (1991). Odor-modulated upwind flight of the sphinx moth, *Manduca sexta* L. *J. comp. Physiol.* A **169**, 427–440.

WILLIS, M. A., MURLIS, J. AND CARDÉ, R. T. (1991). Pheromone-mediated upwind flight of male gypsy moths, *Lymantria dispar*, in a forest. *Physiol. Ent.* **16**, 507–521.

WINET, H. (1973). Wall drag on free-moving ciliated micro-organisms. *J. exp. Biol.* **59**, 753–766.